

involve

a journal of mathematics

A mathematical model of treatment of
cancer stem cells with immunotherapy

Zachary J. Abernathy and Gabrielle Epelle



A mathematical model of treatment of cancer stem cells with immunotherapy

Zachary J. Abernathy and Gabrielle Epelle

(Communicated by Kenneth S. Berenhaut)

Using the work of Shelby Wilson and Doron Levy (2012), we develop a mathematical model to study the growth and responsiveness of cancerous tumors to various immunotherapy treatments. We use numerical simulations and stability analysis to predict long-term behavior of passive and aggressive tumors with a range of antigenicities. For high antigenicity aggressive tumors, we show that remission is only achieved after combination treatment with TGF- β inhibitors and a peptide vaccine. Additionally, we show that combination treatment has limited effectiveness on low antigenicity aggressive tumors and that using TGF- β inhibition or vaccine treatment alone proves generally ineffective for all tumor types considered. A key feature of our model is the identification of separate cancer stem cell and tumor cell populations. Our model predicts that even with combination treatment, failure to completely eliminate the cancer stem cell population leads to cancer recurrence.

1. Introduction

Cancer is a leading cause of death in the world today. Although an enormous amount of resources have been spent in search of a cure, much is still unknown about the dynamics of how cancer cells are created and destroyed. The general consensus is that cancer is caused by mutated cells, which are unable to die and thus grow uncontrollably, and that cancer requires many mutations to transform normal cells into cancer cells [Li and Neaves 2006]. However, another theory of cancer development, which states that cancer arises from stem cells, is steadily gaining recognition.

MSC2010: 34D05, 34D20, 92B05, 92C37.

Keywords: cancer stem cells, immunotherapy, recurrence, ordinary differential equations, stability.

1.1. *Stem cells and cancer.* The cancer stem cell hypothesis originated in 1855 when German pathologist Rudolf Virchow theorized that cancers arise from the activation of inactive embryonic-like cells found in mature tissue [Huntly and Gilliland 2005]. In 1994, John Dick's lab showed the presence of leukemia-inducing stem cells in the blood of mice with acute myeloid leukemia. In 2003 and 2004, Michael Clarke's and Peter Dirks' labs showed the presence of cancer stem cells in breast and brain cancer respectively [Li and Neaves 2006].

Cancer stem cells differ from other tumor cells in their potential for growth, development and differentiation. Unlike other cells, cancer stem cells have the ability to self-renew. A cancer stem cell divides to produce two daughter cells. One daughter remains a stem cell while the other mutates and undergoes further differentiation. Cancer stem cells also have a higher potential for proliferation and a longer life span than other cells [Li and Neaves 2006].

1.2. *Treatment of cancer stem cells.* Another difference between cancer stem cells and other tumor cell types is their resistance to radiation and chemotherapy. Although these treatments are able to destroy the differentiated tumor cells, they are relatively ineffective against cancer stem cells, which have mechanisms for repairing DNA and resisting cytotoxic drugs [Deonarain et al. 2009]. Even if such treatments cause the patient to go into remission, in many cases the cancer relapses months or years later due to the presence of cancer stem cells [Cripe et al. 2009]. Further complicating matters is the fact that chemotherapy and radiation have a greater effect on normal cells than cancerous cells. Research shows that chemotherapy and radiation cause normal hematopoietic stem cells, but not cancer stem cells, to undergo senescence or premature aging. This gives the cancer cells a growth advantage over normal cells, especially after several rounds of treatment [Jordan et al. 2006].

1.2.1. *Immunotherapy.* Immunotherapy is a form of treatment that aims to improve the ability of the immune system to fight cancer cells [Stewart and Smyth 2011]. One of the major advantages of immunotherapy over traditional cancer treatments, such as radiation and chemotherapy, is that the immune system is much more discriminatory in its actions, targeting only cancer cells and leaving the majority of the healthy tissues of the body unharmed [Joshi et al. 2009]. This lessens the competitive advantage of cancer stem cells over normal stem cells after successive rounds of treatment. Paul Ehrlich, an immunologist in the early 20th century, was the first person to conceive the idea that the immune system is capable of scanning for and eradicating the tumors that arise in our bodies before they become clinically manifested [Malmberg 2004]. Although this idea was controversial at first, experimental evidence has shown that when cancer cells proliferate to a detectable number within the human body, the body's immune system is activated into a "search and destroy" mode. This spontaneous immune response is possible only if

the cancer cells have unique surface markers called tumor specific antigens. Tumor cells that possess these antigens are known as immunogenic cancers [Nani and Freedman 2000]. The recognition of cancerous cells by the immune system is called immune surveillance, and cancer progression occurs when this process fails [Stewart and Smyth 2011].

1.2.2. TGF- β : an agent of both tumor suppression and progression. Transforming growth factor- β (TGF- β) is a protein that acts as a strong inhibitor of cell growth and an inducer of programmed cell death or apoptosis [Akhurst and Derynck 2001]. TGF- β is present in both normal and tumor cells. It plays a beneficial role in wound healing, inflammation, and angiogenesis (i.e., new blood vessel formation) [Arciero et al. 2004]. At early stages of tumorigenesis, for example, when the tumor is still benign, TGF- β acts directly on cancer cells to suppress tumor growth [Akhurst and Derynck 2001]. However, as time elapses, genetic changes allow TGF- β to stimulate tumor progression by its activities on both the cancerous and nonmalignant structural cell types of the tumor. Experimental evidence has shown that small tumors produce little or no TGF- β , while large tumors produce large amounts of TGF- β and rely heavily on its angiogenesis-promoting and immunosuppressive effects.

The discovery of TGF- β 's immunosuppressive effects has led scientists to implement new forms of treatment aimed to inhibit TGF- β production. Unfortunately, several studies demonstrate that TGF- β inhibition alone is not enough to eliminate tumors. For instance, in [Terabe et al. 2009], the authors examined whether the inhibition of TGF- β can enhance immune responses caused by a peptide vaccine. Their goal was to ascertain under which conditions this enhanced tumor response slows down or stops tumor growth in mice. They found that treatment with only anti-TGF- β had no impact on tumor growth, but anti-TGF- β did greatly enhance the effects of the peptide vaccine. Shelby Wilson and Doron Levy [2012] then developed a mathematical model in order to quantitatively study the results of Terabe et al. Our model modifies the Wilson–Levy model in order to study the effects of TGF- β inhibition and vaccine combination treatment on cancer stem cells.

2. The Wilson–Levy model

We first present the original Wilson–Levy model for proper context. The model follows the size of a tumor represented by $T(t)$, the concentration of TGF- β represented by $G(t)$, the number of effector cells represented by $E(t)$, the number of regulatory T cells represented by $R(t)$, and the number of additional T cells in a vaccine represented by $V(t)$. Note that we relabel the constant d from their paper as d_0 to avoid confusion with the differential operator. Wilson and Levy's model

[2012] is written as the following system of ordinary differential equations:

$$\frac{dT}{dt} = a_0T(1 - c_0T) - \delta_0 \frac{ET}{1 + c_1B} - \delta_0TV, \quad (1)$$

$$\frac{dB}{dt} = a_1 \frac{T^2}{c_2 + T^2} - d_0B, \quad (2)$$

$$\frac{dE}{dt} = \frac{fET}{1 + c_3TB} - rE - \delta_0RE - \delta_1E, \quad (3)$$

$$\frac{dR}{dt} = rE - \delta_1R, \quad (4)$$

$$\frac{dV}{dt} = g(t) - \delta_1V. \quad (5)$$

Equation (1) describes the growth rate of the tumor measured in mm^2 . The tumor is assumed to grow logistically with a growth rate of a_0 and a carrying capacity of $1/c_0$. The second term of (1) represents the rate at which the effector cells are able to destroy tumor cells. The term $1 + c_1B$ represents the negative effect that TGF- β production has on the effector cells' ability to attack the tumor cells. The last term represents the action of the vaccine on the tumor cells.

Equation (2) represents the rate of change in the concentration of TGF- β measured in ng/ml. The switch in the amount of TGF- β production between small and large tumors is modeled by the first term in (2). The constant c_2 represents the tumor cell population at which the switch occurs and a_1 is the maximum rate of TGF- β production [Arciero et al. 2004]. The decay rate for TGF- β is given by d_0 .

Equation (3) represents the rate of change of the number of effector cells in the system. The first term represents the rate at which effector cells are recruited to attack the tumor. The expression $1 + c_3TB$ represents the negative effect of both TGF- β production and tumor growth on the effector cells' ability to proliferate. The constant f represents the tumor's antigenicity and it measures the degree that the tumor is able to stimulate an immune response. The number r represents the rate at which effector cells differentiate into regulatory T cells. The effector cells are also removed when interacting with regulatory T cells at a rate of δ_0 .

Equation (4) represents the number of regulatory T cells in the system. This model assumes that only CD8+ effector cells become regulatory T cells.

Equation (5) represents the rate of change of the vaccine, which is modeled as an addition of 5000 activated T cells at day 3. If the vaccine is given, $g(t)$ is a constant multiple of a Dirac delta function centered at $t = 3$, i.e., $g(t) = g_0\delta(t - 3)$, where $g_0 = 5000$. If the vaccine is withheld, $g(t)$ is identically 0. Finally, the effector cells, regulatory T cells, and activated T cells in the vaccine are all assumed to share a natural death rate of δ_1 .

3. The modified model

We modify Wilson and Levy's equations by modeling the rate of change of cancer stem cells and tumor cells separately in order to better understand how the proposed treatments affect each population. To highlight the role that TGF- β plays in tumor growth and immunosuppression, we follow the example of [Arciero et al. 2004] and choose to consider two scenarios of tumor development, namely:

- passive tumors that do not produce TGF- β ,
- aggressive tumors that produce TGF- β .

3.1. Passive tumor model. In the passive tumor model, we follow the size of the cancer stem cell population represented by $C(t)$, the size of the tumorous cell population represented by $T(t)$, the number of effector cells represented by $E(t)$, and the number of T cells in the vaccine represented by $V(t)$. Our model is written as the following system of ordinary differential equations:

$$\frac{dC}{dt} = kC \left(1 - \frac{C}{M_1} \right) - hEC - hCV, \quad (6)$$

$$\frac{dT}{dt} = kC \frac{C}{M_1} \left(1 - \frac{T}{M_2} \right) - hET - hTV - d_1T, \quad (7)$$

$$\frac{dE}{dt} = fET - rE - d_3E, \quad (8)$$

$$\frac{dV}{dt} = g(t) - d_3V. \quad (9)$$

Note that $G = 0$ in the passive tumor case, as these tumors do not produce TGF- β . Equation (6) describes the growth rate of the cancer stem cells of the tumor, which are assumed to follow logistic growth with a growth rate of k and a carrying capacity of M_1 . The term hEC represents the rate at which effector cells attack the C stem cells.

Equation (7) represents the growth rate of the tumor cells. The fraction of C stem cells that differentiate into T tumor cells is represented by C/M_1 , and we assume that the tumor cells are nondividing. Hence, if $C < M_1$, then some of the stem cells will produce more stem cells, while other stem cells will produce tumor cells. If $C = M_1$, then all of the stem cells will produce tumor cells. This behavior reflects normal stem cell dynamics [Soltysova et al. 2005]. The carrying capacity of tumor cells is given by M_2 , and we assume the tumor cells have a small natural death rate of d_1 . The term hET represents the rate at which effector cells attack the tumor cells. We assume that the effector cells are able to attack the C and T cells at the same rate. Similarly, the terms hCV and hTV represent the detrimental effect that

the vaccine has on both the C and T cells, and we assume that the vaccine is equally effective against C and T cells.

Equations (8) and (9) model the effector cells and vaccine and follow directly from equations (3) and (5), where we have ignored the contributions of regulatory T cells as they only slightly increase the rate of decay of the effector cells and thus do not greatly affect the dynamics of the model. We relabel the death rate of the effector cells and vaccine as d_3 .

3.2. Aggressive tumor model. Our model of aggressive tumors is represented by the following system of ordinary differential equations:

$$\frac{dC}{dt} = kC \left(1 - \frac{C}{M_1} \right) - h \frac{EC}{1 + c_1 B} - hCV, \quad (10)$$

$$\frac{dT}{dt} = kC \frac{C}{M_1} \left(1 - \frac{T}{M_2} \right) - h \frac{ET}{1 + c_1 B} - hTV - d_1 T, \quad (11)$$

$$\frac{dB}{dt} = a \frac{C^2}{c_2 + C^2} - d_2 B, \quad (12)$$

$$\frac{dE}{dt} = \frac{fET}{1 + c_3 TB} - rE - d_3 E, \quad (13)$$

$$\frac{dV}{dt} = g(t) - d_3 V. \quad (14)$$

Equations (10), (11), (13) and (14) follow directly from the passive tumor model, with the corresponding adjustments made to the interaction terms involving the effector cells E in accordance with the Wilson–Levy model. Equation (12) represents the rate at which TGF- β is produced by the tumor. We assume that TGF- β is only produced by cancer stem cells. There is a growing body of medical evidence that shows the link between TGF- β production and cancer stem cells [Dreesen and Brivanlou 2007; Tang et al. 2008; Mishra et al. 2005].

4. Simulations

In order to better understand the behavior of our models, we perform numerical simulations using Mathematica 9's `NDSolve` command. The code used will be made available upon request. All of our simulations are measured in days. We simulate the growth of four types of tumors, namely:

- (1) low antigenicity passive tumors (LAPTs),
- (2) high antigenicity passive tumors (HAPTs),
- (3) low antigenicity aggressive tumors (LAATs),
- (4) high antigenicity aggressive tumors (HAATs).

	value	units	description
k	0.18	days ⁻¹	tumor growth rate
h	10 ⁻⁵	# ⁻¹ days ⁻¹	vaccine/effector cell-induced tumor death rate
M_1	40	mm ²	cancer stem cell carrying capacity
M_2	369	mm ²	tumor cell carrying capacity
d_1	10 ⁻⁹	days ⁻¹	death rate of tumor cells
f	low: 5 · 10 ⁻⁶ high: 0.05	(mm ²) ⁻¹ days ⁻¹	tumor antigenicity
r	0.01	days ⁻¹	effector cell removal rate to regulatory T cells
d_3	10 ⁻⁵	days ⁻¹	vaccine/effector cell death rate
g_0	5000	# days ⁻¹	additional T cells provided by vaccine

Table 1. Parameters for passive tumor model.

4.1. Simulation of the passive tumor model. Table 1 lists the values of the parameters used in the passive tumor model. All parameter values are taken from Wilson and Levy with the exception of f and k , which are taken from Kirschner and Panetta, and M_1 and d_1 , which are estimated based on the expected low ratio of cancer stem cells to tumor cells and slow natural death rate of tumor cells. A parameter sensitivity analysis is conducted in Section 7 to assess sensitivity of the model to these parameter values. Following the example of Wilson and Levy, we assume that there are 100 effector T cells present at the initial time point in all cases except for the high antigenicity passive tumors, in which we assume that there are 1000 effector T cells present (see discussion below). We choose 0.7 and 3 mm² as our initial stem cell and tumor cell sizes, respectively. The simulations for passive tumor growth with no treatment for both low and high antigenicities are presented in Figure 1.

In Figure 1, the graphs in the top row show the low antigenicity of the tumor does not prompt a response from the effector cells, and thus both the C stem cells and T tumor cells grow to their respective carrying capacities while the number of E effector cells at the tumor site decays over time. In contrast, the graphs in the bottom row of Figure 1 show the behavior of a passive tumor with high antigenicity. In this case, the effector cells undergo an oscillatory response and begin to restrict the tumor's growth. There is biological evidence to support these oscillations in cancers such as chronic myeloid leukemia [Kirschner and Panetta 1998]. While both the C and T cell populations continue to persist, the effector cells reduce the steady-state population size of each cancer cell type to very minute levels.

4.2. Simulation of the aggressive tumor model. We next present the behavior of our aggressive tumor model for both low and high antigenicities. In Table 2, we introduce the new parameter values used in the aggressive tumor model. As before, all

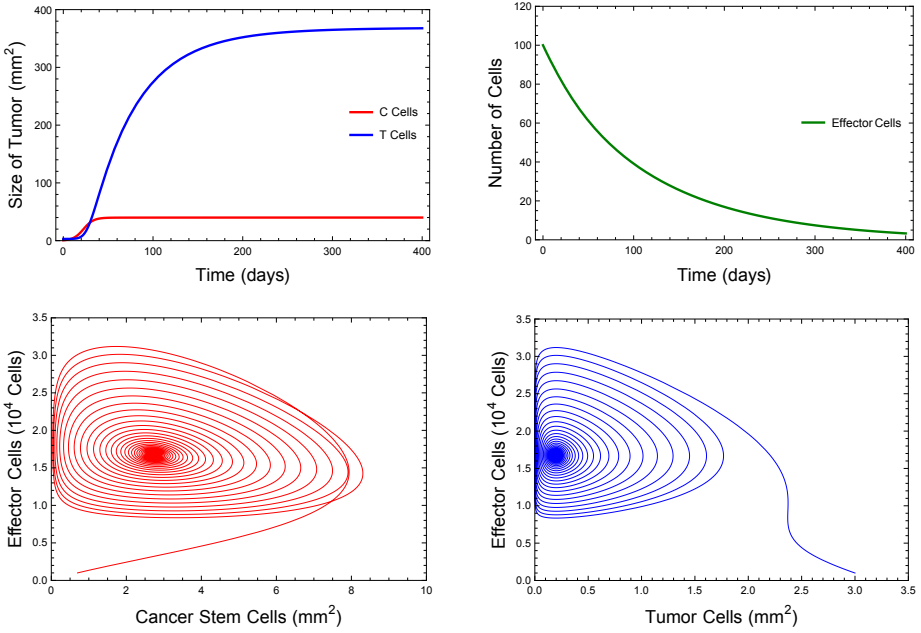


Figure 1. Passive tumor simulations. The graphs in the top row model a tumor with low antigenicity and those in the bottom row model one with high antigenicity.

	value	units	description
k	0.1946	days ⁻¹	tumor growth rate
M_1	40	mm ²	cancer stem cell carrying capacity
M_2	369	mm ²	tumor cell carrying capacity
h	10^{-5}	# ⁻¹ days ⁻¹	vaccine/effector cell-induced tumor death rate
c_1	100	ml/ng	TGF- β inhibition of effector cell-induced tumor death
d_1	10^{-9}	days ⁻¹	death rate of tumor cells
a	0.3	days ⁻¹ ng/ml	maximum rate of TGF- β production
c_2	300	(mm ²) ²	steepness coefficient of TGF- β production
d_2	$7 \cdot 10^{-4}$	days ⁻¹	rate of degradation of TGF- β
f	low: $5 \cdot 10^{-6}$ high: 0.62	(mm ²) ⁻¹ days ⁻¹	tumor antigenicity
c_3	300	ml/(ng mm ²)	tumor cell and TGF- β inhibition of effector cell activation
r	0.01	# ⁻¹	effector cell removal rate to regulatory T cells
d_3	10^{-5}	days ⁻¹	vaccine/effector cell death rate
g_0	5000	# days ⁻¹	additional T cells provided by vaccine

Table 2. Parameters for aggressive tumor model.

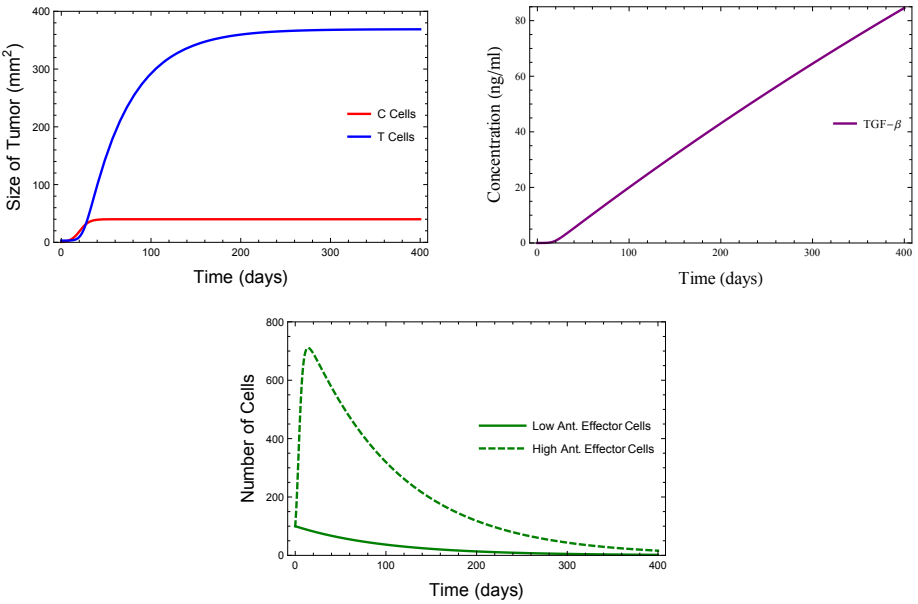


Figure 2. Aggressive tumor simulations.

values are taken from Wilson and Levy (including the slightly higher tumor growth rate k and antigenicity f) with the exception of M_1 and d_1 , which are estimated as stated above. The initial conditions for the cancer stem cell, tumor cell, and effector cell populations remain unchanged, and we use 0.0035 ng/ml as the initial concentration of TGF- β produced by the tumor. Figure 2 shows the results of our simulations for the aggressive tumor model with no treatment. In Figure 2, top left, the C cancer stem cells and T tumor cells grow uninterrupted to their carrying capacities for both low and high antigenicity levels. Similarly, Figure 2, top right, shows the concentration of TGF- β produced by the C stem cells steadily increases regardless of antigenicity level. The only discernible difference with respect to antigenicity occurs with the effector cell population in Figure 2, bottom, where an initial spike in the number of effector cells is seen in the high antigenicity case. However, due to the inhibitory effect of TGF- β on the effector cell population, this increase is short-lasting and the effector cell population decays over time, failing to halt tumor progression.

5. Treatment

Following the example of [Wilson and Levy 2012], we divide treatment into three cases in order to test their relative effectiveness on both the C and T cells, namely:

- vaccine treatment,
- TGF- β inhibition,
- combination treatment.

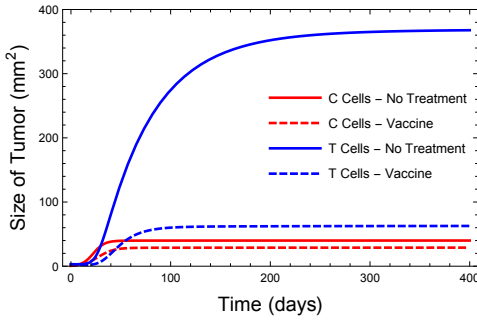


Figure 3. Vaccine treatment for LAPT_s.

5.1. Treatment of passive tumors. Since passive tumors do not produce $\text{TGF-}\beta$, we consider only vaccine treatment, which is modeled by the introduction of 5000 effector cells on day 3 of simulation. Figure 3 shows the results of the vaccine treatment for a low antigenicity passive tumor.

The vaccine treatment is successful in reducing the final steady states of both the cancer stem cells and tumor cells, but cannot clear the tumor entirely. The evolution of the effector cell population is unaffected by the vaccine treatment, and the effector cells decay as in Figure 1, top right. For high antigenicity passive tumors, the vaccine treatment produces no noticeable difference in either the C , T , or E cell dynamics over time, leading to simulations identical to those found in the graphs in the bottom row of Figure 1. The large oscillatory response of the effector cells dominates any contribution from the vaccine in diminishing the cancer cell populations.

5.2. Treatment of aggressive tumors. With the inclusion of $\text{TGF-}\beta$ production by cancer stem cells in aggressive tumors, we now have all three treatment options to consider.

5.2.1. Vaccine treatment. We begin by repeating the vaccine treatment simulation for low and high antigenicity aggressive tumors, shown in Figure 4.

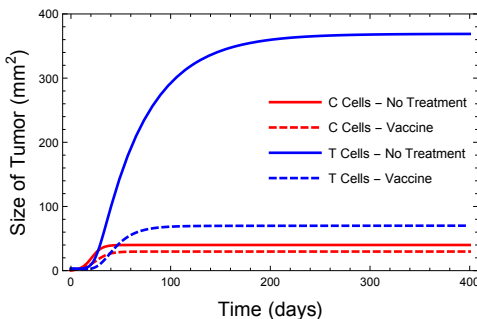


Figure 4. Vaccine treatment for LAAT_s and HAAT_s.

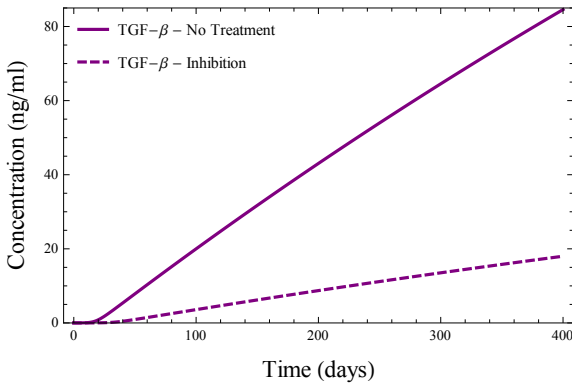


Figure 5. TGF- β Inhibition for LAATs and HAATs.

For both antigenicity levels, the steady states of the cancer stem cells and tumor cells are diminished by the vaccine, similar to the vaccine treatment of the low antigenicity passive tumor. No appreciable difference is observed in the effector cells or TGF- β concentration of the aggressive tumor model under the vaccine. For a more accurate comparison between the effects of treatment in Figures 3 and 4, the size of the C cell population at day 400 for the low antigenicity passive tumor is approximately 28.9 mm^2 and for the low/high antigenicity aggressive tumor is approximately 29.7 mm^2 . Similarly, the size of the T cell population at day 400 is 62.7 mm^2 for the low antigenicity passive tumor and 70.1 mm^2 for the low/high antigenicity aggressive tumor.

5.2.2. TGF- β inhibition. As in [Wilson and Levy 2012], TGF- β inhibition is modeled as an increase of c_2 from 300 to 7000. For both low and high antigenicity tumors, TGF- β inhibition has a nearly negligible effect on the final tumor size, with the C and T cells growing to their carrying capacities as in Figure 2, top left. While the treatment succeeds in slowing down TGF- β production by the tumor (see Figure 5), it fails to lead to any measurable reduction in cancer growth.

As a final note, while the effector cells continue to decay normally for low antigenicity tumors (as in Figure 2, bottom), the TGF- β inhibition induces a large initial response of the effector cells for high antigenicity tumors (see Figure 6). Nevertheless, the effector cells have little impact on tumor growth in this case.

5.2.3. Combination treatment. Again following [Wilson and Levy 2012], combination treatment is modeled by both the increase in c_2 from 300 to 7000 and the administration of the vaccine. For low antigenicity tumors, the combination treatment reduces the C and T steady-state populations to the same levels as the vaccine treatment alone, with no noticeable benefit from adding the TGF- β inhibition. For high antigenicity tumors, on the other hand, the combination treatment is highly effective, reducing both the C and T populations to nearly zero by approximately

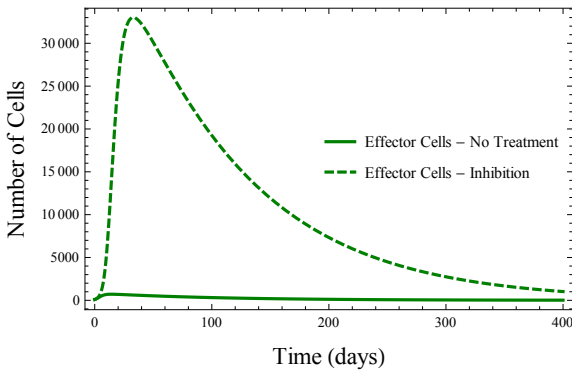


Figure 6. Effector cells under TGF- β inhibition for HAATs.

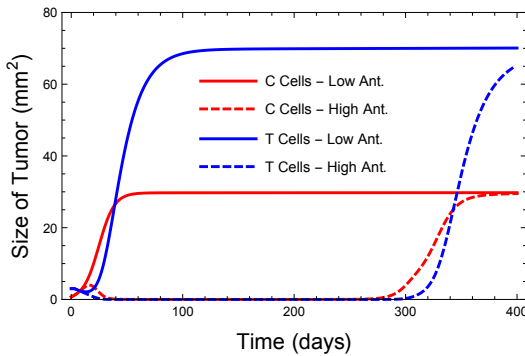


Figure 7. Combination treatment for LAATs and HAATs.

day 30. However, the remission is temporary and both cancer cell populations start growing again shortly before day 300 (see Figure 7).

In Figure 8, the effector cell population also displays new behavior under the combination treatment for high antigenicity tumors. The treatment produces a

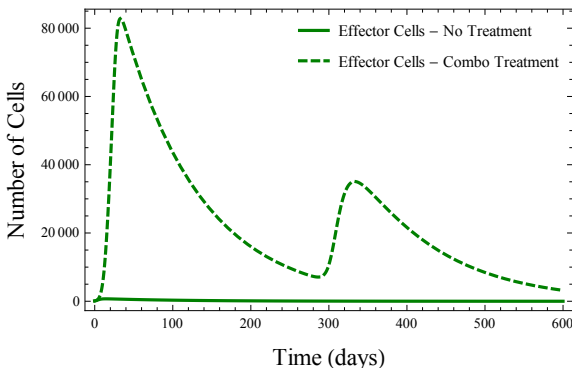


Figure 8. Effector cells under combination treatment for HAATs.

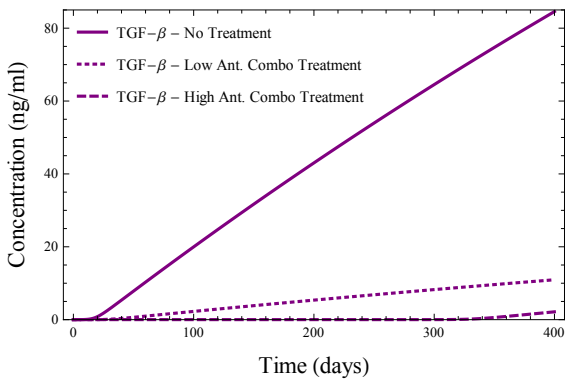


Figure 9. TGF-β concentration under combination treatment for LAATs and HAATs.

significant initial spike in effector cells, helping send the cancer into its temporary remission. Once the cancer begins to recur around day 300, the effector cells produce a second smaller response that is unable to slow the cancer’s growth. Finally, the suppression of TGF-β production by the C cancer stem cells under combination treatment is shown in Figure 9. For high antigenicity tumors in particular, the concentration of TGF-β is greatly diminished for the first year of simulated time.

5.2.4. Summary of simulations. Table 3 provides a summary of the behavior of the treatment outcomes on all four types of tumors. In general, our simulations reveal

	no treatment	vaccine	TGF-β inhibition	combination
LAPT	C, T cells grow to CC; no E cell response	(C, T) = (72%, 17%) of CC at end	not applicable	not applicable
HAPT	C, T cells reduced to minute levels; E cells produce large oscillatory response		not applicable	not applicable
LAAT	C, T cells grow to CC; no E cell response	(C, T) = (74%, 19%) of CC at end	C, T cells grow to CC; no E cell response	(C, T) = (74%, 19%) of CC at end
HAAT	C, T cells grow to CC; small initial E cell response	(C, T) = (74%, 19%) of CC at end	C, T cells grow to CC; large initial E cell response	C, T cells reduced to nearly 0; recurrence by day 300; very large initial E cell response with secondary response when cancer recurs

Table 3. Summary of treatment outcomes for four types of tumors.

that the vaccine treatment is overall more effective than TGF- β inhibition at combating cancer growth. The cancer stem cells appear more resilient to the additional effector cells provided by the vaccine, with a smaller reduction in carrying capacity when compared with the tumor cells. Also, the largest effect of TGF- β inhibition is seen when combined with the vaccine against high antigenicity aggressive tumors, sending the cancer into remission for an extended period of time.

6. Stability analysis

6.1. Dimensionless models. To reduce the number of parameters in the model and ease calculations, we follow the example of [Kirschner and Panetta 1998; Arciero et al. 2004] and nondimensionalize our equations using the following scaling:

$$x = \frac{C}{M_1}, \quad y = \frac{T}{M_2}, \quad z = c_1 B, \quad w = \frac{hE}{r}, \quad v = \frac{d_3 V}{g_0},$$

$$\tau = kt, \quad \rho = \frac{r}{k}, \quad \eta = \frac{hg_0}{kd_3}, \quad \mu = \frac{M_1}{M_2}, \quad \alpha = \frac{ac_1}{k},$$

$$\beta = \frac{c_2}{M_1^2}, \quad \gamma = \frac{M_2 f}{k}, \quad \sigma = \frac{M_2 c_3}{c_1}, \quad \delta_1 = \frac{d_1}{k}, \quad \delta_2 = \frac{d_2}{k}, \quad \delta_3 = \frac{d_3}{k}.$$

This results in the following scaled system of differential equations for the passive tumor model:

$$\frac{dx}{d\tau} = x(1-x) - \rho wx - \eta xv, \quad (15)$$

$$\frac{dy}{d\tau} = \mu x^2(1-y) - \rho wy - \eta yv - \delta_1 y, \quad (16)$$

$$\frac{dw}{d\tau} = \gamma wy - \rho w - \delta_3 w, \quad (17)$$

$$\frac{dv}{d\tau} = \delta_3 \delta (\tau - 3k) - \delta_3 v. \quad (18)$$

Similarly, the scaled aggressive tumor model is given by:

$$\frac{dx}{d\tau} = x(1-x) - \rho \frac{wx}{1+z} - \eta xv, \quad (19)$$

$$\frac{dy}{d\tau} = \mu x^2(1-y) - \rho \frac{wy}{1+z} - \eta yv - \delta_1 y, \quad (20)$$

$$\frac{dz}{d\tau} = \frac{\alpha x^2}{\beta + x^2} - \delta_2 z, \quad (21)$$

$$\frac{dw}{d\tau} = \gamma \frac{wy}{1 + \sigma yz} - \rho w - \delta_3 w, \quad (22)$$

$$\frac{dv}{d\tau} = \delta_3 \delta (\tau - 3k) - \delta_3 v. \quad (23)$$

6.2. Stability of passive tumor model. In order to assess the stability of the passive tumor model, we first find equilibrium solutions by setting (15)–(18) equal to 0 and solving the resulting nonlinear algebraic system of equations. Note that the long-term behavior of the vaccine is clearly exponential decay to zero, so we set $v = 0$ for the remainder of the analysis to simplify the calculation of the other equilibrium populations. Mathematica 9 produces five equilibrium points for the remaining x , y , and w populations, one of which contains a negative component and is thus not biologically meaningful, and two interior equilibrium points whose closed form is too complex to analyze. The other two equilibria that we are able to study are

$$P_1 : (x, y, w) = (0, 0, 0),$$

$$P_2 : (x, y, w) = \left(1, \frac{\mu}{\delta_1 + \mu}, 0\right).$$

Next, we calculate the Jacobian matrix with $v = 0$:

$$\begin{pmatrix} \partial f/\partial x & \partial f/\partial y & \partial f/\partial w \\ \partial g/\partial x & \partial g/\partial y & \partial g/\partial w \\ \partial h/\partial x & \partial h/\partial y & \partial h/\partial w \end{pmatrix},$$

where

$$f(x, y, w) = x(1 - x) - \rho wx,$$

$$g(x, y, w) = \mu x^2(1 - y) - \rho wy - \delta_1 y,$$

$$h(x, y, w) = \gamma wy - \rho w - \delta_3 w.$$

By substituting each equilibrium point into the above Jacobian, a quick calculation of the eigenvalues of the resulting matrix reveals that the origin P_1 is always unstable, while the second equilibrium point P_2 is stable if and only if

$$\rho + \delta_3 > \frac{\gamma\mu}{\delta_1 + \mu}. \quad (24)$$

Biologically, this inequality indicates that if the removal rate of the effector cells is too high relative to the tumor's antigenicity and size, then the effector cells will provide an insufficient response to halt tumor growth and will eventually decay to zero. Testing the parameters for the passive tumor model in Table 1, we find that for low antigenicity passive tumors,

$$\rho + \delta_3 = 0.0556, \quad \frac{\gamma\mu}{\delta_1 + \mu} = 0.01025.$$

Hence inequality (24) is satisfied and P_2 is stable, supporting the behavior observed in Figure 1, top row. On the other hand, for high antigenicity passive tumors we have

$$\rho + \delta_3 = 0.0556, \quad \frac{\gamma\mu}{\delta_1 + \mu} = 102.5.$$

Thus P_2 is unstable in this case. To further investigate the long-term behavior of high antigenicity passive tumors, we may substitute the parameters from [Table 1](#) into the symbolically intractable interior equilibrium points. We find that there is indeed a third positive equilibrium point P_3 , namely $(x, y, w) = (0.0683, 0.00054, 16.7705)$, corresponding to steady-state populations of $C = 2.732$, $T = .2002$, and $E = 16770.5$. Additionally, all three eigenvalues of the Jacobian matrix for this equilibrium have negative real part, two of which come in a complex conjugate pair. Hence P_3 is stable, and the complex-valued eigenvalues provide evidence for the oscillatory behavior seen in [Figure 1](#), bottom row.

6.3. Stability of aggressive tumor model. Following the procedure of the previous section, we set (19)–(23) equal to 0 to search for steady-state solutions of the aggressive tumor model. Mathematica 9 returns seven equilibrium solutions, but due to the highly nonlinear nature of the model, again only two permit a local stability analysis:

$$A_1 : (x, y, z, w) = (0, 0, 0, 0),$$

$$A_2 : (x, y, z, w) = \left(1, \frac{\mu}{\delta_1 + \mu}, \frac{\alpha}{(1 + \beta)\delta_2}, 0\right).$$

The Jacobian matrix of the system with $v = 0$ now has the form

$$\begin{pmatrix} \partial f/\partial x & \partial f/\partial y & \partial f/\partial z & \partial f/\partial w \\ \partial g/\partial x & \partial g/\partial y & \partial g/\partial z & \partial g/\partial w \\ \partial h/\partial x & \partial h/\partial y & \partial h/\partial z & \partial h/\partial w \\ \partial j/\partial x & \partial j/\partial y & \partial j/\partial z & \partial j/\partial w \end{pmatrix},$$

where

$$f(x, y, z, w) = x(1 - x) - \rho \frac{wx}{1 + z},$$

$$g(x, y, z, w) = \mu x^2(1 - y) - \rho \frac{wy}{1 + z} - \delta_1 y,$$

$$h(w, x, y, z) = \frac{\alpha x^2}{\beta + x^2} - \delta_2 z,$$

$$j(x, y, z, w) = \gamma \frac{wy}{1 + \sigma yz} - \rho w - \delta_3 w.$$

By calculating the eigenvalues of the Jacobian at each equilibrium point, it is easily seen that the origin A_1 is again unstable, while the second equilibrium point A_2 is stable if and only if

$$\rho + \delta_3 > \frac{(1 + \beta)\gamma\mu\delta_2}{\alpha\mu\sigma + (1 + \beta)(\delta_1 + \mu)\delta_2}. \tag{25}$$

This inequality establishes a threshold for the removal rate of effector cells in terms of tumor antigenicity, size, and TGF- β production that, if exceeded, results in exponential decay of the effector cells and growth of the cancer stem cell and tumor cell populations to their carrying capacities. Using the parameters found in Table 2 for the aggressive tumor model, a quick calculation as before reveals that inequality (25) is satisfied for both low and high antigenicity aggressive tumors. Hence A_2 is stable in both cases, matching our earlier observations in Figure 2.

7. Sensitivity analysis

In order to assess the sensitivity of our model to changes in parameters, we conduct a sensitivity analysis for combination treatment of high antigenicity aggressive tumors. More specifically, we vary each parameter over a range of percentages centered around a baseline for 365 simulated days while leaving all other parameters fixed and observe the effects on the resulting T tumor cell population. The results are presented in Figure 10. In contrast with the findings in [Wilson and Levy 2012], while the antigenicity f ranked high among the most sensitive parameters, we find that there are three more sensitive parameters: the cancer growth rate k , the initial injection of T cells by the vaccine g_0 , and the carrying capacity of the cancer stem cells M_1 . It will thus be crucial to obtain highly accurate biological estimates for these parameters to increase the applicability of the model.

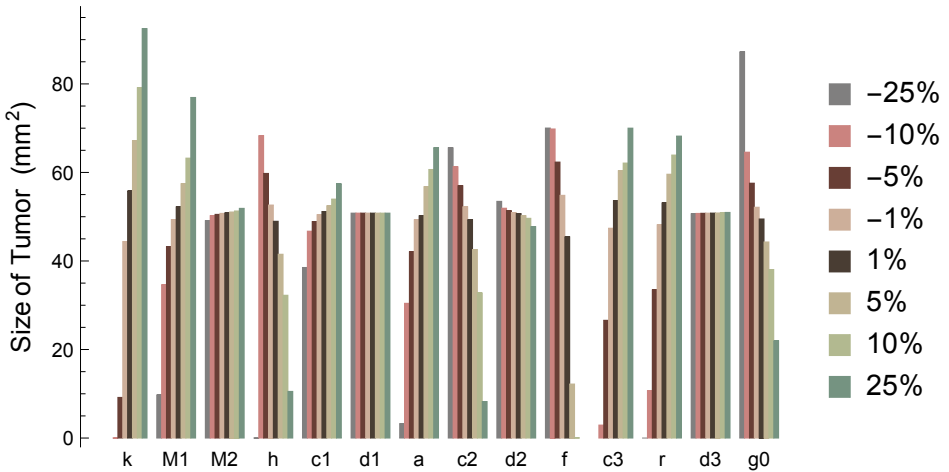


Figure 10. Sensitivity analysis for HAATs. Baseline values: $k = 0.1946$, $M_1 = 40$, $M_2 = 369$, $h = 10^{-5}$, $c_1 = 100$, $d_1 = 10^{-9}$, $a = 0.3$, $c_2 = 7000$, $d_2 = 7 \cdot 10^{-4}$, $f = 0.62$, $c_3 = 300$, $r = 0.01$, $d_3 = 10^{-5}$, $g_0 = 5000$.

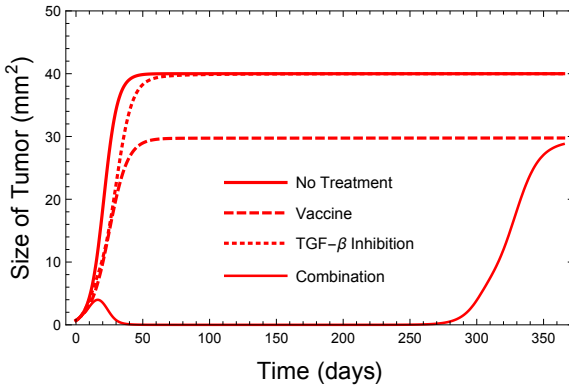


Figure 11. Response of cancer stem cells to treatment.

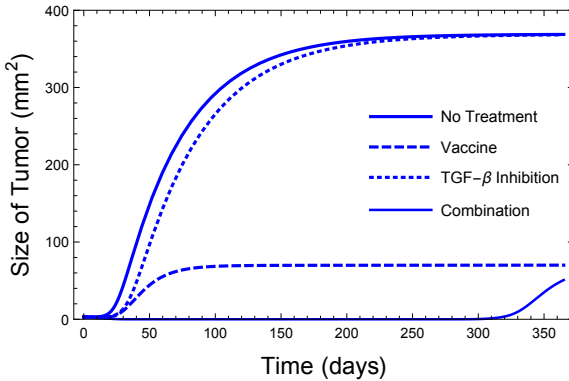


Figure 12. Response of tumor cells to treatment.

8. Results

Figures 11 and 12 show the relative effectiveness of the vaccine, TGF- β inhibition, and combination treatments against the C and T cell populations of a high antigenicity aggressive tumor, respectively.

Although TGF- β inhibition moderately slows down tumor growth in both cases, the C stem cells are able to reach their carrying capacity by approximately day 60, while the T tumor cells reach their carrying capacity by day 250. Alternatively, in the vaccine treatment case, the vaccine is able to reduce the tumor cell population from its carrying capacity of 369 mm^2 to 70.1 mm^2 (a reduction of 81%), while it is only able to reduce the stem cell population from its carrying capacity of 40 mm^2 to 29.7 mm^2 (a reduction of 16%). Although remission is achieved in our simulations of combination treatment, from Figure 11 we can see that the stem cell population is not completely destroyed and as a result, the cancer stem cells reemerge by day 250 and prompt renewed growth of the tumor cells by day 300. Our results agree with

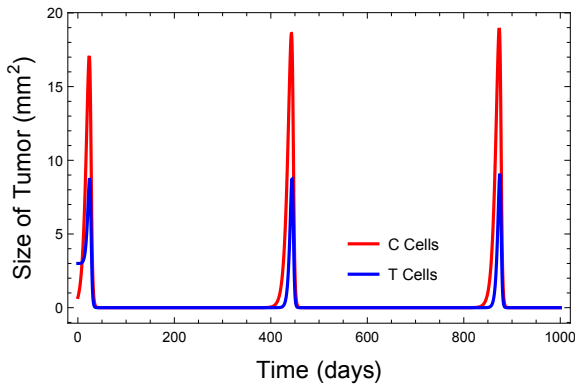


Figure 13. Cancer cells approaching limit cycle for HAPT.

studies that show that unless cancer treatment is specifically directed toward cancer stem cells, the cancer can still recur, even if there is a significant reduction in tumor size after treatment [Jordan et al. 2006].

Conversely, in our simulation of low antigenicity aggressive tumors we show that although combination treatment succeeds in reducing the size of the tumor, it is unable to eliminate either the C or T cell populations. Furthermore, in our simulations of treatment of passive tumors, we find that the vaccine produces a similar outcome for low antigenicity tumors. The effector cell response for high antigenicity passive tumors is sufficient to significantly reduce final tumor size, and the vaccine treatment produces no noticeable benefit for this type of tumor.

The oscillatory behavior seen in our passive tumor model deserves further mention. In [Kirschner and Panetta 1998], the authors find that in the no treatment case, as they increase tumor antigenicity, the long-term dynamics of their model transition from a stable node to a stable limit cycle to a stable spiral. It is interesting to observe that in our model, the progression of these dynamics as the antigenicity increases occurs in a somewhat different manner. Keeping all other values in Table 1 fixed, for $f < 2.71 \cdot 10^{-5}$, the equilibrium point P_2 is a stable node, as in Figure 1, top row. Biologically speaking, this implies that extremely low antigenicity tumors are able to effectively escape immunosurveillance and grow to carrying capacity. For $2.71 \cdot 10^{-5} < f < 1.13 \cdot 10^{-4}$, P_2 becomes unstable and one of the interior equilibria becomes a stable node. Next, for $1.14 \cdot 10^{-4} < f < 0.0856$, the positive interior equilibrium transitions to a stable spiral. Thus all cell populations begin to oscillate, and the effector cells reduce the size of the tumor to nearly zero before the oscillations eventually dampen out. Finally, for $f > 0.0857$, the interior equilibrium becomes an unstable spiral and the cell populations oscillate without bound.

Moreover, for $f > 0.0445$, a stable limit cycle is created. Thus for the high antigenicity value used in our passive tumor model, $f = 0.05$, the long-term

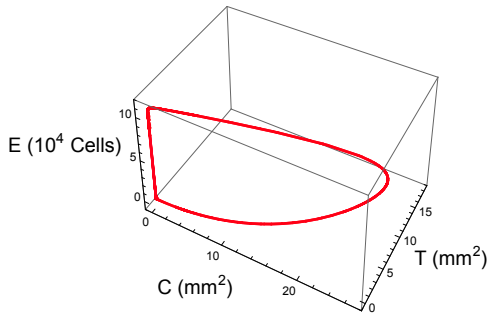


Figure 14. Limit cycle in phase space for HAPT.

dynamics either result in damped or sustained oscillations, depending on the initial conditions. For example, if we let $f = 0.05$ and the initial population of effector cells satisfy $E(0) = 100$, then the cell populations indeed approach the stable limit cycle. A plot of the cancer cell populations in this case is shown in [Figure 13](#), and the limit cycle in phase space is presented in [Figure 14](#).

However, if $E(0) = 1000$, we find that the populations approach the interior stable spiral. This behavior was demonstrated in [Figure 1](#), bottom row, for our high antigenicity passive tumors.

9. Discussion

The mathematical model presented in this paper describes the dynamics of cancer stem cells, tumor cells, and effector cells under one or more treatment protocols designed to elicit a larger than normal response from the body's natural immune system. The antigenicity of the tumor as well as the aggressiveness of the tumor via TGF- β production play a crucial role in predicting the success of such techniques. We find that a vaccine delivering additional effector cells is able to diminish the size of highly antigenic tumors, and pairing the vaccine with a TGF- β inhibitor can lead to at least temporary clearance of aggressive tumors. As expected, low antigenic tumors are able to better evade immunosurveillance and persist in the face of immunotherapy techniques, with aggressive tumors of this type being particularly resistant to treatment. For these tumors, other treatment options such as chemotherapy and radiation therapy should be explored.

Qualitatively, the behavior of our model for high antigenicity aggressive tumors agrees with the results of the Wilson–Levy model, with remission only being achieved after combination treatment. However, our model is additionally able to show how each of the various treatments affect the cancer stem cell and tumor cell populations individually. We show that the cancer stem cells are more resistant to the vaccine and experience a smaller reduction in carrying capacity when compared to the tumor cells. In addition the re-emergence of the tumor in all cases of

treatment of high antigenicity aggressive tumors also agrees with the stability analysis presented by Wilson and Levy [2012], which predicts that all treatment scenarios will eventually lead to a nonzero tumor equilibrium.

Furthermore, our simulations of passive tumors agree strongly with the results of Arciero et al., with low antigenic tumors escaping the immune response and growing to carrying capacity, while increasing antigenicity leads to damped oscillations that stabilize into a small persistent tumor. The behavior of aggressive tumors with low and high antigenicity in both models is also similar. The Arciero et al. model [2004] simulates siRNA treatment designed to suppress TGF- β expression in tumor cells, and as with our TGF- β inhibition strategy, they find that such a strategy alone is insufficient to clear aggressive tumors.

Future research will include further study of the global behavior of the model, including stability analysis of internal equilibria and identification of the basins of attraction for various equilibria and limit cycles. The parameters of the model should additionally be fit to experimental data to obtain a more biologically realistic time-scale for the dynamics predicted by the model. Lastly, the model suggests that inclusion of treatment methods that specifically target cancer stem cells could potentially lead to tumor clearance, even for aggressive low antigenic tumors. This possibility warrants further research by both mathematicians and biologists alike.

References

- [Akhurst and Derynck 2001] R. J. Akhurst and R. Derynck, “TGF- β signaling in cancer: a double-edged sword”, *Trends Cell Bio.* **11**:11 (2001), S44–S51.
- [Arciero et al. 2004] J. C. Arciero, T. L. Jackson, and D. E. Kirschner, “A mathematical model of tumor-immune evasion and siRNA treatment”, *Discrete Contin. Dyn. Syst. Ser. B* **4**:1 (2004), 39–58. [MR](#) [Zbl](#)
- [Cripe et al. 2009] T. P. Cripe, P.-Y. Wang, P. Marcato, Y. Y. Mahller, and P. W. K. Lee, “Targeting cancer-initiating cells with oncolytic viruses”, *Molecular Therapy* **17**:10 (2009), 1677–1682.
- [Deonarain et al. 2009] M. P. Deonarain, C. A. Kousparou, and A. A. Epenetos, “Antibodies targeting cancer stem cells: a new paradigm in immunotherapy?”, *Mabs* **1**:1 (2009), 12–25.
- [Dreesen and Brivanlou 2007] O. Dreesen and A. H. Brivanlou, “Signaling pathways in cancer and embryonic stem cells”, *Stem Cell Rev.* **3**:1 (2007), 7–17.
- [Huntly and Gilliland 2005] B. J. P. Huntly and D. G. Gilliland, “Leukaemia stem cells and the evolution of cancer-stem-cell research”, *Nat. Rev. Cancer* **5**:4 (2005), 311–321.
- [Jordan et al. 2006] C. T. Jordan, M. L. Guzman, and M. Noble, “Cancer stem cells”, *New Eng. J. Med.* **355**:12 (2006), 1253–1261.
- [Joshi et al. 2009] B. Joshi, X. Wang, S. Banerjee, H. Tian, A. Matzavinos, and M. A. J. Chaplain, “On immunotherapies and cancer vaccination protocols: a mathematical modelling approach”, *J. Theor. Biol.* **259**:4 (2009), 820–827. [MR](#)
- [Kirschner and Panetta 1998] D. Kirschner and J. C. Panetta, “Modeling immunotherapy of the tumor-immune interaction”, *J. Math. Biol.* **37**:3 (1998), 235–252. [Zbl](#)

- [Li and Neaves 2006] L. Li and W. B. Neaves, “Normal stem cells and cancer stem cells: the niche matters”, *Cancer Res.* **66**:9 (2006), 4553–4557.
- [Malmberg 2004] K.-J. Malmberg, “Effective immunotherapy against cancer”, *Cancer Immunology, Immunotherapy* **53**:10 (2004), 879–892.
- [Mishra et al. 2005] L. Mishra, K. Shetty, Y. Tang, A. Stuart, and S. W. Byers, “The role of TGF- β and Wnt signaling in gastrointestinal stem cells and cancer”, *Oncogene* **24**:37 (2005), 5775–5789.
- [Nani and Freedman 2000] F. Nani and H. I. Freedman, “A mathematical model of cancer treatment by immunotherapy”, *Math. Biosci.* **163**:2 (2000), 159–199. MR Zbl
- [Soltysova et al. 2005] A. Soltysova, V. Altanerova, and C. Altaner, “Cancer stem cells”, *Neoplasma* **52**:6 (2005), 435–440.
- [Stewart and Smyth 2011] T. J. Stewart and M. J. Smyth, “Improving cancer immunotherapy by targeting tumor-induced immune suppression”, *Cancer Metastasis Rev.* **30**:1 (2011), 125–140.
- [Tang et al. 2008] Y. Tang, K. Kitisin, W. Jogunoori, C. Li, C.-X. Deng, S. C. Mueller, H. W. Ransom, A. Rashid, A. R. He, J. S. Mendelson, J. M. Jessup, K. Shetty, M. Zaslloff, B. Mishra, E. P. Reddy, L. Johnson, and L. Mishra, “Progenitor/stem cells give rise to liver cancer due to aberrant TGF- β and IL-6 signaling”, *Proc. Nat. Acad. Sci.* **105**:7 (2008), 2445–2450.
- [Terabe et al. 2009] M. Terabe, E. Ambrosino, S. Takaku, J. J. O’Konek, D. Venzon, S. Lonning, J. M. McPherson, and J. A. Berzofsky, “Synergistic enhancement of CD8+ T cell-mediated tumor vaccine efficacy by an anti-transforming growth factor- β monoclonal antibody”, *Clin. Cancer Res.* **15**:21 (2009), 6560–6569.
- [Wilson and Levy 2012] S. Wilson and D. Levy, “A mathematical model of the enhancement of tumor vaccine efficacy by immunotherapy”, *Bull. Math. Biol.* **74**:7 (2012), 1485–1500. MR Zbl

Received: 2014-09-02

Revised: 2016-04-21

Accepted: 2017-06-27

abernathy@winthrop.edu

Department of Mathematics, Winthrop University,
Rock Hill, SC, United States

epelleg2@winthrop.edu

Department of Mathematics, Winthrop University,
Rock Hill, SC, United States

INVOLVE YOUR STUDENTS IN RESEARCH

Involve showcases and encourages high-quality mathematical research involving students from all academic levels. The editorial board consists of mathematical scientists committed to nurturing student participation in research. Bridging the gap between the extremes of purely undergraduate research journals and mainstream research journals, *Involve* provides a venue to mathematicians wishing to encourage the creative involvement of students.

MANAGING EDITOR

Kenneth S. Berenhaut Wake Forest University, USA

BOARD OF EDITORS

Colin Adams	Williams College, USA	Suzanne Lenhart	University of Tennessee, USA
John V. Baxley	Wake Forest University, NC, USA	Chi-Kwong Li	College of William and Mary, USA
Arthur T. Benjamin	Harvey Mudd College, USA	Robert B. Lund	Clemson University, USA
Martin Bohner	Missouri U of Science and Technology, USA	Gaven J. Martin	Massey University, New Zealand
Nigel Boston	University of Wisconsin, USA	Mary Meyer	Colorado State University, USA
Amarjit S. Budhiraja	U of North Carolina, Chapel Hill, USA	Emil Minchev	Ruse, Bulgaria
Pietro Cerone	La Trobe University, Australia	Frank Morgan	Williams College, USA
Scott Chapman	Sam Houston State University, USA	Mohammad Sal Moslehian	Ferdowsi University of Mashhad, Iran
Joshua N. Cooper	University of South Carolina, USA	Zuhair Nashed	University of Central Florida, USA
Jem N. Corcoran	University of Colorado, USA	Ken Ono	Emory University, USA
Toka Diagana	Howard University, USA	Timothy E. O'Brien	Loyola University Chicago, USA
Michael Dorff	Brigham Young University, USA	Joseph O'Rourke	Smith College, USA
Sever S. Dragomir	Victoria University, Australia	Yuval Peres	Microsoft Research, USA
Behrouz Emamizadeh	The Petroleum Institute, UAE	Y.-F. S. Pétermann	Université de Genève, Switzerland
Joel Foisy	SUNY Potsdam, USA	Robert J. Plemmons	Wake Forest University, USA
Erin W. Fulp	Wake Forest University, USA	Carl B. Pomerance	Dartmouth College, USA
Joseph Gallian	University of Minnesota Duluth, USA	Vadim Ponomarenko	San Diego State University, USA
Stephan R. Garcia	Pomona College, USA	Bjorn Poonen	UC Berkeley, USA
Anant Godbole	East Tennessee State University, USA	James Propp	U Mass Lowell, USA
Ron Gould	Emory University, USA	József H. Przytycki	George Washington University, USA
Andrew Granville	Université Montréal, Canada	Richard Rebarber	University of Nebraska, USA
Jerrold Griggs	University of South Carolina, USA	Robert W. Robinson	University of Georgia, USA
Sat Gupta	U of North Carolina, Greensboro, USA	Filip Saidak	U of North Carolina, Greensboro, USA
Jim Haglund	University of Pennsylvania, USA	James A. Sellers	Penn State University, USA
Johnny Henderson	Baylor University, USA	Andrew J. Sterge	Honorary Editor
Jim Hoste	Pitzer College, USA	Ann Trenk	Wellesley College, USA
Natalia Hritonenko	Prairie View A&M University, USA	Ravi Vakil	Stanford University, USA
Glenn H. Hurlbert	Arizona State University, USA	Antonia Vecchio	Consiglio Nazionale delle Ricerche, Italy
Charles R. Johnson	College of William and Mary, USA	Ram U. Verma	University of Toledo, USA
K. B. Kulasekera	Clemson University, USA	John C. Wierman	Johns Hopkins University, USA
Gerry Ladas	University of Rhode Island, USA	Michael E. Zieve	University of Michigan, USA

PRODUCTION

Silvio Levy, Scientific Editor


Cover: Alex Scorpan

See inside back cover or msp.org/involve for submission instructions. The subscription price for 2018 is US \$190/year for the electronic version, and \$250/year (+\$35, if shipping outside the US) for print and electronic. Subscriptions, requests for back issues and changes of subscriber address should be sent to MSP.

Involve (ISSN 1944-4184 electronic, 1944-4176 printed) at Mathematical Sciences Publishers, 798 Evans Hall #3840, c/o University of California, Berkeley, CA 94720-3840, is published continuously online. Periodical rate postage paid at Berkeley, CA 94704, and additional mailing offices.

Involve peer review and production are managed by EditFlow® from Mathematical Sciences Publishers.

PUBLISHED BY

 **mathematical sciences publishers**
nonprofit scientific publishing

<http://msp.org/>

© 2018 Mathematical Sciences Publishers

involve

2018

vol. 11

no. 3

A mathematical model of treatment of cancer stem cells with immunotherapy	361
ZACHARY J. ABERNATHY AND GABRIELLE EPELLE	
RNA, local moves on plane trees, and transpositions on tableaux	383
LAURA DEL DUCA, JENNIFER TRIPP, JULIANNA TYMOCZKO AND JUDY WANG	
Six variations on a theme: almost planar graphs	413
MAX LIPTON, EOIN MACKALL, THOMAS W. MATTMAN, MIKE PIERCE, SAMANTHA ROBINSON, JEREMY THOMAS AND ILAN WEINSCHELBAUM	
Nested Frobenius extensions of graded superrings	449
EDWARD POON AND ALISTAIR SAVAGE	
On G-graphs of certain finite groups	463
MOHAMMAD REZA DARAFSHEH AND SAFOORA MADADY MOGHADAM	
The tropical semiring in higher dimensions	477
JOHN NORTON AND SANDRA SPIROFF	
A tale of two circles: geometry of a class of quartic polynomials	489
CHRISTOPHER FRAYER AND LANDON GAUTHIER	
Zeros of polynomials with four-term recurrence	501
KHANG TRAN AND ANDRES ZUMBA	
Binary frames with prescribed dot products and frame operator	519
VERONIKA FURST AND ERIC P. SMITH	